In silico evaluation of the pharmacological properties of 1,2,4-triazolo[1’,5’:1,6]pyrido[3,4-b]indole derivatives

S. O. Fedotov[A,B,C,D], A. S. Hotsulia[E,F]

Zaporizhzhia State Medical and Pharmaceutical University, Ukraine

A – research concept and design; B – collection and/or assembly of data; C – data analysis and interpretation; D – writing the article; E – critical revision of the article; F – final approval of the article

The condensed 1,2,4-triazolo[1′,5′:1,6]pyrido[3,4-*b*]indole scaffold, combining indole and 1,2,4-triazole pharmacophores, represents a promising source of anti-inflammatory, antimicrobial and anticancer agents. *In silico* assessment of their toxicity, pharmacokinetics and molecular properties provides a rational basis for synthesis and biological evaluation.

The aim of this study is to apply *in silico* approaches to investigate the physicochemical, pharmacokinetic and toxicological properties of 1,2,4-triazolo-[1′,5′:1,6]pyrido[3,4-*b*]indole derivatives and to explore their potential as multitarget agents through molecular docking.

Materials and methods. The pharmacological properties of 1,2,4-triazolo[1′,5′:1,6]pyrido[3,4-*b*]indole derivatives were evaluated using *in silico* modeling approaches. Toxicity prediction was performed with the US EPA TEST software package, while physicochemical and pharmacokinetic parameters were assessed using SwissADME. Molecular docking was conducted to analyze ligand interactions with cyclooxygenase-2, lanosterol 14α-demethylase, peptide deformylase of *E. coli* and *S. aureus* and anaplastic lymphoma kinase.

Results. The 1,2,4-triazolo[1′,5′:1,6]pyrido[3,4-*b*]indole derivatives were characterized by moderate oral toxicity and low mutagenic risk, except for compounds **1** and **5**. Drug-likeness analysis confirmed compliance with criteria for orally active agents, while ADME modeling indicated high gastrointestinal absorption, limited central nervous system penetration (except compound **10**) and potential CYP450 interactions. Docking studies revealed strong binding to COX-2 and CYP51, with compounds **2**, **5**, **8** and **10** showing affinities comparable to fluconazole. Several derivatives also exceeded actinonin in binding to *E. coli* peptide deformylase and displayed diverse interactions with *S. aureus* PDF. Compounds **2**, **5** and **10** demonstrated binding energies against ALK close to crizotinib.

Overall, these findings suggest favorable pharmacokinetic profiles and multitarget potential for anti-inflammatory, antimicrobial and anticancer applications, with lipophilicity and CYP450 interactions identified as possible limitations.

Conclusions. *In silico* modeling demonstrated that 1,2,4-triazolo[1′,5′:1,6]pyrido[3,4-*b*]indole derivatives possess favorable pharmacokinetic properties, relatively low predicted toxicity, and strong affinities toward multiple pharmacologically relevant targets. These findings provide a rationale for further experimental validation and the development of novel multitarget drug candidates.

Keywords: 1,2,4-triazole, indole, in silico study, properties.

Current issues in pharmacy and medicine: science and practice. 2025;18(3):253-263

Оцінювання in silico фармакологічних властивостей похідних 1,2,4-тріазоло[1’,5’:1,6]піридо[3,4-b]індолу

С. О. Федотов, А. С. Гоцуля

Конденсований скелет 1,2,4-тріазоло[1′,5′:1,6]піридо[3,4-*b*]індолу, який поєднує фармакофори індолу та 1,2,4-тріазолу, є перспективним джерелом протизапальних, протимікробних і протипухлинних агентів. *In silico* оцінювання їхньої токсичності, фармакокінетики та молекулярних властивостей дає раціональну основу для синтезу та біологічного дослідження.

Мета роботи – застосування *in silico* підходів для вивчення фізико-хімічних, фармакокінетичних і токсикологічних властивостей похідних 1,2,4-тріазоло[1′,5′:1,6]піридо[3,4-*b*]індолу та дослідження їхнього потенціалу як мультитаргетних агентів шляхом молекулярного докінгу.

Матеріали і методи. Фармакологічні властивості похідних 1,2,4-тріазоло[1′,5′:1,6]піридо[3,4-*b*]індолу оцінювали за допомогою *in silico* моделювання. Прогноз токсичності здійснювали з використанням програмного пакета TEST Агентства з охорони довкілля США, а фізико-хімічні та фармакокінетичні параметри – за допомогою онлайн-платформи SwissADME. Молекулярний докінг здійснювали для аналізу взаємодії лігандів із циклооксигеназою-2, ланостерол 14α-деметилазою, пептиддеформілазою *E. coli* та *S. aureus*, а також анапластичною лімфомною кіназою.

ARTICLE INFO

UDC 547.792’821’752:615.015.11]-047.44:004.94
DOI: 10.14739/2409-2932.2025.3.338994

Current issues in pharmacy and medicine: science and practice. 2025;18(3):253-263

Keywords: 1,2,4-triazole, indole, in silico study, properties.

Received: 16.07.2025 // Revised: 22.09.2025 // Accepted: 24.09.2025

Результати. Похідні 1,2,4-тріазоло[1′,5′:1,6]піридо[3,4-*b*]індолу характеризувалися помірною оральною токсичністю та низьким мутагенним ризиком, крім сполук **1** і **5**. Аналіз подібності до лікарських засобів підтвердив відповідність критеріям для перорально активних агентів, а моделювання ADME показало високу шлунково-кишкову абсорбцію, обмежене проникнення у центральну нервову систему (крім сполуки **10**) та потенційні взаємодії з CYP450. Дослідження докінгу показали сильне зв'язування з COX-2 і CYP51, причому сполуки **2**, **5**, **8** і **10** мали афінність, зіставну з флуконазолом. Декілька похідних також перевищували актінонін за здатністю зв'язуватися з пептиддеформілазою *E. coli* і мали різні взаємодії з PDF *S. aureus*. Сполуки **2**, **5** і **10** показали енергії зв'язування з ALK, близькі до кризотинібу.

Результати дослідження дали змогу встановити сприятливі фармакокінетичні профілі та мультитаргетний потенціал із векторним спрямуванням протизапальної, протимікробної та протипухлинної активності, а ліпофільність і взаємодії з CYP450 визначено як можливі обмеження.

Висновки. *In silico* моделювання показало, що похідні 1,2,4-тріазоло[1′,5′:1,6]піридо[3,4-*b*]індолу мають сприятливі фармакокінетичні властивості, відносно низьку передбачувану токсичність і сильну афінність до кількох фармакологічно значущих мішеней. Одержані дані є основою для подальшої експериментальної верифікації та розробки нових мультитаргетних лікарських кандидатів.

Ключові слова: 1,2,4-тріазол, індол, in silico дослідження, властивості.

Актуальні питання фармацевтичної і медичної науки та практики. 2025. Т. 18, № 3(49). С. 253-263

Modern strategies for the discovery of biologically active compounds increasingly rely on *in silico* methods, which provide a rapid and relatively accurate assessment of the pharmacological and toxicological properties of potential candidates [1,2,3]. The use of computer modeling at the early stages of drug development makes it possible to significantly reduce the scope of experimental studies, to lower financial costs, and to minimize risks associated with the synthesis of ineffective or toxic molecules.

One of the promising directions in contemporary medicinal chemistry is the investigation of condensed heterocyclic systems that combine several pharmacophoric fragments within their structure [4,5]. Derivatives of 1,2,4-triazole are characterized by a wide range of pharmacological effects, including anti-inflammatory, antimicrobial, antitumor and antifungal activities [6,7,8,9,10]. An equally important pharmacophoric component is indole and its condensed derivatives, which serve as a key structural element of many natural and synthetic molecules exhibiting pronounced neurotropic, anticancer and cardioprotective properties.

The combination of indole and 1,2,4-triazole synthons within a single molecule lays the foundation for the development of a promising scaffold for innovative ligands with potential multitarget activity [11]. In this context, particular attention should be paid to 1,2,4-triazolo[1′,5′:1,6]pyrido[3,4-*b*]indole and its derivatives. They integrate the structural features of both pharmacophores and hold significant potential for pharmacological applications.

Aim

The aim of this study is the *in silico* evaluation of the physicochemical, pharmacokinetic and toxicological properties of a series of 1,2,4-triazolo[1′,5′:1,6]pyrido[3,4-*b*]indole derivatives, as well as the assessment of their ability to interact with biological targets through molecular docking.

Materials and methods

The selection of structures for the study was guided by the intrinsic potential of the involved synthons, their consistency with the general principles of organic chemistry, and the achievements of previous research in this field. Considering these factors, 1,2,4-triazolo[1′,5′:1,6]pyrido[3,4-*b*]indole and its derivatives were proposed for *in silico* evaluation of pharmacological potential *(Fig. 1)*. All investigated derivatives are hydrazides of 2-methyl-6,11-dihydro-[1,2,4]triazolo[1′,5′:1,6]pyrido[3,4-*b*]indole, differing in the nature of the aryl substituent at the hydrazone moiety. Among them are compounds with a simple benzylidene fragment (**2**), derivatives bearing methoxy-substituted rings (**3**, **4**), as well as halogen-substituted derivatives – fluorine (**5**), chlorine and fluorine (**6**), and dichloro (**7**). In addition, a compound with an electron-donating dimethylamino-group (**8**) and derivatives with electron-withdrawing nitro-groups at different positions of the benzyl ring (**9**, **10**) were studied. For comparison, the series also includes the parent carbohydrazide without additional aromatic substituents (**1**). This selection of substituents allows the assessment of the influence of electronic and steric effects on the biological activity of the investigated molecules.

Toxicological properties were predicted using the TEST (Toxicity Estimation Software Tool), providing estimates of acute toxicity, ecotoxicity, and mutagenic potential [12]. Physicochemical and pharmacokinetic parameters, including drug-likeness and oral bioavailability, were assessed with the SwissADME platform. Molecular docking was performed to predict ligand conformations within the binding pockets of selected protein targets and to evaluate their binding affinities. Ligand structures were prepared using MarvinSketch 6.3.0, HyperChem 8 and AutoDock Tools 1.5.6. Protein structures were preprocessed with Discovery Studio 4.0 and AutoDock Tools 1.5.6. Flexible docking simulations were conducted with AutoDock Vina. The docking analysis was carried out for cyclooxygenase-2 (COX-2), lanosterol 14α-demethylase (CYP51), peptide deformylase (PDF) from *Escherichia coli* and *Staphylococcus aureus* and anaplastic lymphoma kinase (ALK) [13,14,15,16].

Results

Predicted acute toxicity (rat LD_{50}) values ranged from 545 mg/kg to 970 mg/kg, indicating moderate toxicity *(Table 1)* [12]. The highest safety was observed for compound **7** (LD_{50} = 970 mg/kg), while compound **10** showed the lowest

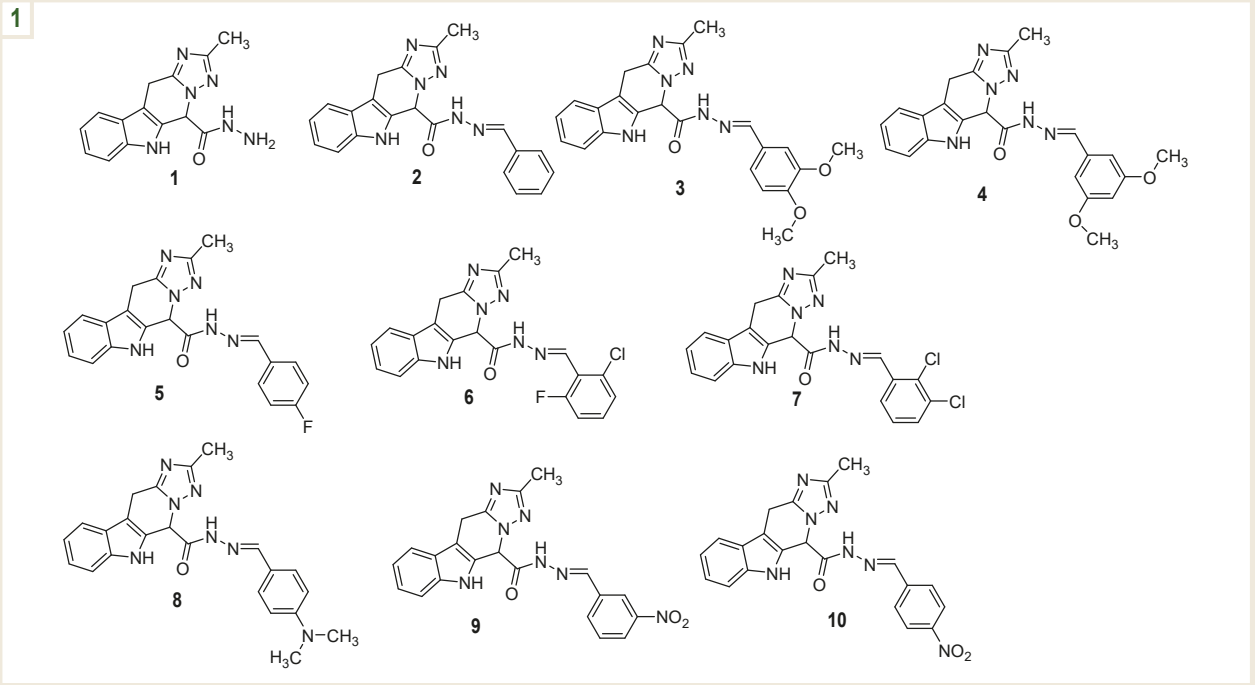

Fig. 1. Model structures for *in silico* studies.

value (LD_{50} = 545 mg/kg). Mutagenicity predictions were negative for most derivatives, except compounds **1** and **5** (positive results).

Based on computer modeling, the predicted LC_{50} values for *Daphnia magna* (48 h) ranged from 1.06 mg/L (**6, 7**) to 32.51 mg/L (**1**). For *Pimephales promelas* (96 h), the predicted LC_{50} values varied between 1.68×10^{-3} mg/L (**7**) and 20.36 mg/L (**1**). Modeling indicated that compounds **6** and **7** may exhibit the highest toxicity (LC_{50} <0.003 mg/L), whereas compound **1** shows markedly lower predicted toxicity values *(Table 1)*.

ADME analysis. Most 1,2,4-triazolo[1′,5′:1,6]pyrido[3,4-*b*] indole derivatives have molecular weights (MW) of 370–440 g/mol, within the acceptable range for oral drugs *(Table 2)*. Compound **1** (282.30 g/mol) may exhibit enhanced permeability and bioavailability.

The number of heavy atoms (HA) and heavy aromatic atoms (HAA) ranges from 28 to 32 and from 14 to 20, respectively. Hydrogen bond acceptors (HBA) range from 4 to 6 and hydrogen bond donors (HBD) from 2 to 3, all values being consistent with drug-likeness criteria. Although slightly above optimal, these parameters are generally acceptable for promising biologically active compounds. The fraction of sp^3 hybridized carbons (Csp^3) of 0.14–0.22 indicates a predominance of aromatic, planar structures, while the number of rotatable bonds (RB) does not exceed six, favoring optimal molecular flexibility.

Molecular refractivity (MR) is ≤120 Å^2 and TPSA ranges from 87.96 to 133.78 Å^2. Compounds **2**, **5–7** (TPSA <90 Å^2) may cross the blood-brain barrier (BBB), whereas compounds **3**, **4** and **10** show higher MR, potentially reducing permeability but favoring interactions with polar targets.

In silico solubility prediction indicated that most of the investigated derivatives (**2–10**) are classified as moderately soluble (MS) according to the ESOL and Ali models, whereas the SILICOS-IT model predicts them as poorly soluble (PS) *(Table 3)*. The only exception is compound **1**, which is classified as soluble (S) in all models, suggesting more favorable pharmacokinetic properties. Predicted Log S values range from -7.88 (**7**) to -2.58 (**1**), corresponding to solubility from $<10^{-5}$ mg/mL to 0.74 mg/mL *(Table 3)*.

Lipophilicity assessment showed that consensus Log $P_{o/w}$ values for most of the investigated compounds range from 0.79 to 3.81, corresponding to moderate to high lipophilicity *(Table 4)*. The highest values were observed for compounds **6** and **7**, consistent with the results of individual models (XLogP3, SILICOS-IT). Compounds **3** and **4** also demonstrated pronounced affinity for lipid environments, whereas derivatives **2**, **5** and **8–10** exhibited moderate lipophilicity. The only hydrophilic compound was **1**, which correlates with its higher predicted aqueous solubility *(Table 4)*.

In silico pharmacokinetic evaluation also indicated a high predicted level of gastrointestinal absorption (GIA), which is favorable for potential oral administration. Only compound **1** was identified as capable of crossing the BBB *(Table 5)*. Assessment of interactions with P-glycoprotein (P-gp) revealed that compounds **1–4**, **8** and **9** are potential P-gp substrates, which may reduce their effective intracellular concentrations due to active efflux. In contrast, compounds **5–7** and **10** showed no indications of P-gp substrate activity.

Analysis of potential interactions with cytochrome P450 enzymes indicated that most compounds (**2–8**, **10**) may inhibit CYP1A2, CYP2C19, and CYP2C9. Additionally, compounds **3**, **4** and **8** demonstrated inhibitory activity toward CYP3A4,

Table 1. Quantitative parameters of *in silico* toxicity assessment

No.	LD_{50} (rats, *per os*), mg/kg / $-\log_{10}$ mol/kg	Mutagenicity	LC_{50} (*Daphnia magna*), 48 hours, $-\log_{10}$ mol/l / mg/l	LC_{50} (*Pimephales promelas*), 96 hours, $\log_{10}$ mol/l / mg/l
1	735 / 0.52	0.52 / +	3.94 / 32.51	4.14 / 20.36
2	630 / 0.26	0.26 / –	5.16 / 2.56	$7.65 / 8.31 \times 10^{-3}$
3	730 / 0.44	0.44 / –	5.38 / 1.81	$7.62 / 1.02 \times 10^{-2}$
4	650 / 0.41	0.41 / –	5.47 / 1.44	$7.63 / 1.02 \times 10^{-2}$
5	675 / 0.60	0.60 / +	5.36 / 1.68	$7.76 / 6.74 \times 10^{-3}$
6	910 / 0.47	0.47 / –	5.60 / 1.06	$8.23 / 2.50 \times 10^{-3}$
7	970 / 0.29	0.29 / –	5.62 / 1.06	$8.42 / 1.68 \times 10^{-3}$
8	706 / 0.37	0.37 / –	5.24 / 2.37	$7.47 / 1.40 \times 10^{-2}$
9	765 / 0.42	–	–	–
10	545 / 0.43	–	–	–

Table 2. Physicochemical properties of the studied compounds

No.	MW, g/mol	HA	HAA	Csp^3	RB	HBA	HBD	MR	TPSA, $Å^2$
1	282.30	21	14	0.21	2	4	3	76.12	101.62
2	370.41	28	20	0.14	4	4	2	106.39	87.96
3	430.46	32	20	0.22	6	6	2	119.38	106.42
4	430.46	32	20	0.22	6	6	2	119.38	106.42
5	388.40	29	20	0.14	4	5	2	106.35	87.96
6	422.84	30	20	0.14	4	5	2	111.36	87.96
7	439.30	30	20	0.14	4	4	2	116.41	87.96
8	413.48	31	20	0.22	5	4	2	120.60	91.20
9	415.40	31	20	0.14	5	6	2	115.21	133.78
10	415.40	31	20	0.14	5	6	2	115.21	133.78

Table 3. Aqueous solubility of the studied compounds

No.	Log S: ESOL	Solubility, – mg/ml; – mol/l	Class	Log S: Ali	Solubility, – mg/ml; – mol/l	Class	Log S: SILICOS-IT	Solubility, – mg/ml; – mol/l	Class
1	-2.58	7.40×10^{-1}; 2.62×10^{-3}	P	-2.72	5.34×10^{-1}; 1.89×10^{-3}	P	-3.79	4.61×10^{-2}; 1.63×10^{-4}	P
2	-4.53	1.09×10^{-2}; 2.95×10^{-5}	MS	-4.91	4.60×10^{-3}; 1.24×10^{-5}	MS	-6.71	7.31×10^{-5}; 1.97×10^{-7}	PS
3	-4.67	9.27×10^{-3}; 2.15×10^{-5}	MS	-5.23	2.53×10^{-3}; 5.87×10^{-6}	MS	-6.91	5.31×10^{-5}; 1.23×10^{-7}	PS
4	-4.67	9.27×10^{-3}; 2.15×10^{-5}	MS	-5.23	2.53×10^{-3}; 5.87×10^{-6}	MS	-6.91	5.31×10^{-5}; 1.23×10^{-7}	PS
5	-4.69	7.99×10^{-3}; 2.06×10^{-5}	MS	-5.01	3.80×10^{-3}; 9.78×10^{-6}	MS	-6.97	4.16×10^{-5}; 1.07×10^{-7}	PS
6	-5.27	2.25×10^{-3}; 5.32×10^{-6}	MS	-5.65	9.40×10^{-4}; 2.22×10^{-6}	MS	-7.56	1.18×10^{-5}; 2.78×10^{-8}	PS
7	-5.71	8.57×10^{-4}; 1.95×10^{-6}	MS	-6.20	2.75×10^{-4}; 6.27×10^{-7}	MP	-7.88	5.83×10^{-6}; 1.33×10^{-8}	PS
8	-4.76	7.25×10^{-3}; 1.75×10^{-5}	MS	-5.10	3.30×10^{-3}; 7.97×10^{-6}	MS	-6.78	6.86×10^{-5}; 1.66×10^{-7}	PS
9	-4.58	1.10×10^{-2}; 2.64×10^{-5}	MS	-5.68	8.65×10^{-4}; 2.08×10^{-6}	MS	-6.05	3.73×10^{-4}; 8.97×10^{-7}	PS
10	-4.58	1.10×10^{-2}; 2.64×10^{-5}	MS	-5.68	8.65×10^{-4}; 2.08×10^{-6}	MS	-6.05	3.73×10^{-4}; 8.97×10^{-7}	PS

Table 4. Lipophilicity of the studied compounds

No.	Log $P_{o/w}$ (iLogP)	Log $P_{o/w}$ (XLogP3)	Log $P_{o/w}$ (WLogP)	Log $P_{o/w}$ (MLogP)	Log $P_{o/w}$ (SILICOS-IT)	Consensus Log $P_{o/w}$
1	1.06	1.00	0.55	0.76	0.56	0.79
2	1.89	3.38	2.71	2.14	3.20	2.66
3	3.02	3.32	2.73	1.54	3.32	2.79
4	3.20	3.32	2.73	1.54	3.32	2.82
5	2.65	3.48	3.27	2.52	3.62	3.11
6	2.13	4.10	3.92	3.00	4.26	3.48
7	2.82	4.63	4.02	3.11	4.48	3.81
8	1.98	3.50	2.78	2.06	2.88	2.64
9	1.38	3.20	2.62	1.29	1.03	1.91
10	2.05	3.20	2.62	1.29	1.03	2.04

Table 5. Pharmacokinetics of the studied compounds

No.	GIA	Crossing the BBB	P-gp substrate	CYP1A2 inhibitor	CYP2C19 inhibitor	CYP2C9 inhibitor	CYP2D6 inhibitor	CYP3A4 inhibitor	Log Kp, cm/s
1	High	–	+	–	+	–	–	–	-7.31
2	High	–	+	+	+	+	–	–	-6.16
3	High	–	+	–	+	+	+	+	-6.57
4	High	–	+	–	+	+	+	+	-6.57
5	High	–	–	+	+	+	–	–	-6.20
6	High	–	–	+	+	+	–	–	-5.97
7	High	–	–	+	+	+	–	–	-5.69
8	High	–	+	–	+	+	–	+	-6.34
9	High	–	+	–	+	+	–	–	-6.56
10	High	–	–	+	+	+	–	–	-6.56

while compounds **3** and **8** also inhibited CYP2D6. In contrast, compound **1** showed no inhibitory effect on any of the studied isoenzymes.

Predicted skin permeability (Log Kp) values for most derivatives ranged from -5.69 cm/s to -7.31 cm/s, corresponding to low to moderate transdermal absorption potential. The lowest values were observed for compounds **3** and **4**, while the highest was recorded for compound **7**.

All investigated compounds complied with Lipinski's rule of five (L), confirming their potential suitability for oral administration. Additionally, all molecules met the criteria of the Ghose (G), Veber (V) and Egan (E) rules. Only compound **1** fully satisfied the Muegge (M) filter, whereas deviations were observed for the remaining derivatives, due to elevated molecular weight (>350 g/mol) and XLogP3 values above 3.5 *(Table 6)*.

Predicted absolute oral bioavailability for all compounds is 0.55. The PAINS (Pan Assay Interference Compounds) filter revealed at least one alert in each investigated compound, associated with the indol-3-yl fragment. This synthon is characteristic of compounds with pronounced biological activity; however, it may also lead to nonspecific interactions in bioassays, thereby increasing the risk of false-positive results.

The Brenk filter identified potentially undesirable fragments from the perspective of chemical reactivity. For compounds **2**–**8**, a single alert was recorded, related to the presence of an imino fragment. Compounds **9** and **10** exhibited several warnings, including imino and nitro groups as well as O–N linkages, which may contribute to their toxicity or chemical instability. Compound **1** displayed two alerts, associated with acylhydrazine and hydrazine fragments, indicating possible reactivity and the need for further toxicological evaluation *(Table 6)*.

Such alerts do not necessarily preclude a compound from further consideration; however, they underscore the necessity of cautious interpretation of its biological activity. During subsequent structural optimization, mitigation strategies may be employed, such as modification or replacement of the "problematic" fragments with less reactive analogues, introduction of electron-donating or electron-withdrawing substituents to stabilize the molecule, or the design of bioisosteres that preserve activity while reducing the risk of nonspecific effects. This approach allows the combination of high bioactivity with improved safety and reliability of bioassay results.

Molecular docking demonstrated that the 1,2,4-triazolo[1′,5′:1,6]pyrido[3,4-*b*]indole derivatives form stable complex-

Table 6. Drug-likeness of the studied compound series

No.	Filter					Alerts	
	L	G	V	I	M	PAINS	Brenk
1	+	+	+	+	+	1	2
2	+	+	+	+	–	1	1
3	+	+	+	+	–	1	1
4	+	+	+	+	–	1	1
5	+	+	+	+	–	1	1
6	+	+	+	+	–	1	1
7	+	+	+	+	–	1	1
8	+	+	+	+	–	1	1
9	+	+	+	–	–	1	3
10	+	+	+	–	–	1	3

Table 7. Intermolecular interaction energies of the studied compounds with COX-2

No.	E_{min}	No.	E_{min}	No.	E_{min}	No.	E_{min}	No.	E_{min}
1	-9.0	**3**	-9.1	**5**	-9.4	**7**	-8.1	**9**	-9.4
2	-8.9	**4**	-9.3	**6**	-9.5	**8**	-8.8	**10**	-9.4
Celecoxib	-13.4								

Table 8. Nature and types of interactions of the studied structures with COX-2

No.	Nature of amino acid residues
1	LEU A:532 (alkyl, π-alkyl), ALA A:528 (π-σ), VAL A:524 (alkyl, π-alkyl), LEU A:385 (alkyl, π-alkyl), LEU A:353 (alkyl, π-alkyl), VAL A:350 (alkyl, π-alkyl), MET A:523 (alkyl, π-alkyl), PHE A:519 (alkyl, π-alkyl), TRP A:388 (alkyl, π-alkyl)
2	VAL A:117 (π-σ), SER A:354 (C–H bond), ALA A:528 (alkyl, π-alkyl), HIS A:90 (alkyl, π-alkyl), VAL A:524 (π-σ), LEU A:353 (alkyl, π-alkyl)
3	ALA A:528 (alkyl, π-alkyl), GLU A:525 (π-anion), VAL A:350 (alkyl, π-alkyl), PHE A:519 (alkyl, π-alkyl), MET A:523 (C–H bond), ARG A:121 (π-σ), SER A:354 (C–H bond), VAL A:524 (alkyl, π-alkyl), VAL A:117 (alkyl, π-alkyl), LEU A:124 (alkyl, π-alkyl), HIS A:90 (alkyl, π-alkyl), TYR A:356 (C–H bond), LEU A:93 (alkyl, π-alkyl), VAL A:89 (alkyl, π-alkyl), TYR A:116 (alkyl, π-alkyl)
4	ALA A:528 (alkyl, π-alkyl), GLU A:525 (π-anion), SER A:354 (C–H bond), TYR A:356 (alkyl, π-alkyl), VAL A:524 (alkyl, π-alkyl), ARG A:121 (π-σ), HIS A:90 (alkyl, π-alkyl), VAL A:350 (alkyl, π-alkyl), LEU A:93 (alkyl, π-alkyl), VAL A:89 (π-σ), VAL A:117 (alkyl, π-alkyl), TYR A:116 (alkyl, π-alkyl)
5	VAL A:350 (alkyl, π-alkyl), ALA A:528 (π-σ), GLU A:525 (π-anion), PRO A:529 (alkyl, π-alkyl), LEU A:124 (alkyl, π-alkyl), ARG A:121 (π-σ), LEU A:532 (alkyl, π-alkyl), VAL A:117 (alkyl, π-alkyl), VAL A:89 (alkyl, π-alkyl), LEU A:93 (alkyl, π-alkyl), TYR A:116 (alkyl, π-alkyl)
6	TYR A:356 (intermolecular H-bond, π–π T-shaped), LEU A:353 (π-σ), VAL A:117 (alkyl, π-alkyl), SER A:354 (C–H bond), VAL A:350 (alkyl, π-alkyl), HIS A:90 (alkyl, π-alkyl), VAL A:524 (π-σ), ALA A:528 (alkyl, π-alkyl), ARG A:514 (π-cation)
7	VAL A:350 (π-σ), ALA A:528 (alkyl, π-alkyl), GLU A:525 (π-anion), ARG A:121 (alkyl, π-alkyl), VAL A:524 (alkyl, π-alkyl), LEU A:353 (alkyl, π-alkyl), TYR A:116 (alkyl, π-alkyl), VAL A:117 (alkyl, π-alkyl), LEU A:93 (alkyl, π-alkyl), VAL A:89 (alkyl, π-alkyl)
8	VAL A:89 (alkyl, π-alkyl), SER A:354 (C–H bond), VAL A:524 (π-σ), TYR A:116 (C–H bond), ALA A:528 (alkyl, π-alkyl), VAL A:350 (alkyl, π-alkyl), LEU A:353 (alkyl, π-alkyl), ALA A:517 (alkyl, π-alkyl)
9	VAL A:524 (C–H bond, π-σ), GLU A:525 (intermolecular interaction forces, π-anion), LEU A:353 (alkyl, π-alkyl), TYR A:356 (alkyl, π-alkyl), LEU A:93 (alkyl, π-alkyl), ALA A:528 (alkyl, π-alkyl), ARG A:121 (π-σ), VAL A:117 (alkyl, π-alkyl), SER A:120 (amide–π stacking)
10	VAL A:350 (π-σ), LEU A:532 (alkyl, π-alkyl), ALA A:528 (π-σ), PRO A:529 (alkyl, π-alkyl), LEU A:124 (alkyl, π-alkyl), GLU A:525 (π-anion), ARG A:121 (π-σ), LEU A:93 (alkyl, π-alkyl), TYR A:116 (alkyl, π-alkyl), VAL A:89 (alkyl, π-alkyl), VAL A:117 (alkyl, π-alkyl)

es with the active site of COX-2 (E_{min} ranging from -8.1 kcal/mol to -9.5 kcal/mol) *(Table 7)*. The highest affinity was observed for compound **6** (-9.5 kcal/mol), with similar values recorded for compounds **4**, **5**, **9** and **10**. For comparison, celecoxib exhibited a markedly lower binding energy (-13.4 kcal/mol).

Molecular docking revealed that the studied compounds establish a broad spectrum of stabilizing interactions with the active site of the COX-2 enzyme. The residues most frequently involved in complex formation include ALA A:528, VAL A:524, VAL A:350, ARG A:121, GLU A:525, LEU A:353, TYR A:116, VAL A:117, LEU A:93, VAL A:89, and SER A:354 *(Table 8)*. The interactions are predominantly hydrophobic (ALA, VAL, LEU), hydrogen-bonding, and electrostatic (ARG, GLU, SER, TYR), which collectively

Table 9. Intermolecular interaction energies of the studied structures with lanosterol 14α-demethylase

No.	E_{min}	No.	E_{min}	No.	E_{min}	No.	E_{min}	No.	E_{min}
1	-8.2	**3**	-9.3	**5**	-11.4	**7**	-9.8	**9**	-10.3
2	-11.1	**4**	-9.8	**6**	-10.5	**8**	-10.9	**10**	-10.6
Fluconazole	-10.9								

Table 10. Nature and types of interactions with lanosterol 14α-demethylase

No.	Types of interactions and amino acid residues
1	LEU A:105 (π-σ), CYS A:394 (conventional H-bond), ALA A:256 (π-σ), ALA A:104 (alkyl, π-alkyl), LEU A:152 (alkyl, π-alkyl), VAL A:395 (alkyl, π-alkyl), LEU A:100 (alkyl, π-alkyl), PHE A:399 (π-π T-shaped)
2	THR A:260 (conventional H bond), LEU A:105 (π-σ), PRO A:320 (π-alkyl), ALA A:400 (π-alkyl), CYS A:394 (conventional H bond), ALA A:256 (π-σ), VAL A:395 (π-σ), LEU A:152 (π-alkyl), LEU A:100 (π-alkyl), ALA A:104(π-alkyl), PHE A:399 (π-π T-shaped)
3	LEU A:315 (alkyl, π-alkyl), ALA A:256 (C-H bond, π-donor H bond), LEU A:324 (π-σ), ALA A:400 (alkyl, π-alkyl), THR A:260 (C-H bond, π-donor H bond), PHE A:387 (alkyl, π-alkyl), PRO A:320 (alkyl, π-alkyl), CYS A:394 (C-H bond, π-donor H bond), THR A:264 (C-H bond, π-donor H bond), LEU A:321 (alkyl, π-alkyl), PHE A:83 (alkyl, π-alkyl), ARG A:96 (Conventional H bond)
4	LEU A:324 (alkyl, π-alkyl), ALA A:256 (C-H bond, π-donor H bond), LEU A:105 (π-σ), LEU A:321 (alkyl, π-alkyl), GLY A:396 (conventional H bond), ALA A:104 (alkyl, π-alkyl), LEU A:152 (alkyl, π-alkyl), CYS A:394 (C-H bond, π-donor H bond), LEU A:100 (alkyl, π-alkyl), PHE A:399 (π-π T-shaped), THR A:260 (C-H bond, π-donor H bond), ALA A:400 (alkyl, π-alkyl)
5	PRO A:320 (alkyl, π-alkyl), THR A:260 (π-σ), LEU A:321 (conventional H bond), ALA A:256 (π-σ), LEU A:152 (alkyl, π-alkyl), PRO A:386 (halogen (Fluorine)), CYS A:394 (alkyl, π-alkyl), VAL A:395 (alkyl, π-alkyl), GLY A:396 (π-σ), LEU A:105 (alkyl, π-alkyl), PHE A:399(π-π T-shaped), ARG A:96 (alkyl, π-alkyl), LEU A:100 (alkyl, π-alkyl)
6	SER A:261 (conventional H bond), ALA A:256 (conventional H bond), CYS A:394 (conventional H bond), PHE A:387 (alkyl, π-alkyl), GLY A:396 (C-H bond), LEU A:321 (π-σ), PRO A:320 (π-σ), THR A:260 (alkyl, π-alkyl), LEU A:324 (alkyl, π-alkyl), LEU A:315(alkyl, π-alkyl)
7	HIS A:259 (π-π T-shaped, π-π stacked), LEU A:321 (alkyl, π-alkyl), LEU A:324 (π-σ), VAL A:434 (alkyl, π-alkyl), MET A:79 (alkyl, π-alkyl), PHE A:78 (π-π T-shaped, π-π Stacked), TYR A:76 (π-σ, alkyl, π-alkyl), LEU A:100 (alkyl, π-alkyl), ALA A:256 (alkyl, π-alkyl), CYS A:394 (conventional H bond), VAL A:395 (alkyl, π-alkyl)
8	ALA A:256 (C-H bond), PHE A:387 (alkyl, π-alkyl), PRO A:320 (alkyl, π-alkyl), LEU A:315 (alkyl, π-alkyl), ALA A:400 (alkyl, π-alkyl), THR A:260 (C-H bond), CYS A:394 (π-S), LEU A:321 (π-σ), TYR A:76 (π-π T-shaped), MET A:79 (alkyl, π-alkyl), SER A:261 (C-H bond), THR A:264 (conventional H bond), VAL A:395 (alkyl, π-alkyl)
9	ARG A:96 (π-donor H bond), LEU A:321 (π-alkyl), TYR A:76 (π-cation), VAL A:395(π-alkyl), PHE A:78 (π-π T-shaped), PHE A:255 (π-alkyl), ALA A:256 (π-alkyl), HIS A:259 (π-alkyl)
10	ALA A:256 (π-σ), GLY A:396 (C-H bond, π-donor H bond), CYS A:394 (π-S), LEU A:324 (alkyl, π-alkyl), LEU A:321 (π-σ), PRO A:320 (alkyl, π-alkyl), ALA A:400 (alkyl, π-alkyl), THR A:260 (C-H bond, π-donor H bond), PHE A:387 (π-π T-shaped, amide-π stacked), GLY A:388 (van der Waals)

stabilize the ligand within the hydrophobic pocket of COX-2. This interaction pattern is consistent with published data, according to which alanine, leucine, tyrosine and valine residues actively participate in binding with inhibitors in the COX-2 hydrophobic pocket. Such a binding mode is characteristic of known COX-2 inhibitors and further supports the relevance of the obtained findings [1]. Based on the number of predicted interactions, compounds **1**, **3–5**, **7** and **9** were the most prominent, suggesting high stability of the respective complexes. Conversely, compounds **2** and **6** exhibited fewer contacts but compensated through the presence of specific interactions, such as hydrogen bonds or π-cation interactions *(Table 8)*.

The investigated compounds formed stable complexes with lanosterol 14α-demethylase (E_{min} -8.2 kcal/mol to -11.4 kcal/mol). The highest binding affinity was observed for compound **5** (-11.4 kcal/mol), surpassing fluconazole (-10.9 kcal/mol); comparable values were obtained for compounds **2, 6** and **8–10**. The remaining compounds demonstrated moderate affinity (-8.2 kcal/mol to -9.8 kcal/mol) *(Table 9)*.

The primary types of interactions between the derivatives and the active site of lanosterol 14α-demethylase (CYP51) were hydrophobic contacts (alkyl, π-alkyl, π-σ), which predominated in most complexes involving LEU A:321, LEU A:324, LEU A:315, LEU A:152, ALA A:256, VAL A:395 and adjacent residues *(Table 10)*. A significant number of compounds also formed aromatic interactions (π-π stacking, T-shaped) with PHE A:78, PHE A:399, TYR A:76, PHE A:387 and HIS A:259, as well as hydrogen bonds with CYS A:394, SER A:261, THR A:260, ARG A:96, and other amino acids. Specific interactions (π-cation, π-S, halogen bond, amide-π stacking, van der Waals interactions) further contributed to the energetic profile of individual complexes. The residues most frequently involved in intermolecular interactions were ALA A:256, LEU A:321, LEU A:324, VAL A:395, CYS A:394 and PHE A:399, forming the functional core of the active site. The most interaction-rich profiles were observed for compounds **2**, **5**, **8** and **10**, with compound **5** exhibiting the greatest diversity of contacts, consistent with its lowest binding energy (-11.4 kcal/mol).

Molecular docking of the 1,2,4-triazolo[1′,5′:1,6]pyrido[3,4-*b*]indole derivatives to the active site of *E. coli* peptide deformylase (PDF) revealed the formation of stable complexes with E_{min} ranging from -6.7 kcal/mol to -7.9 kcal/mol *(Table 11)*. The highest binding affinities were observed for

Table 11. Intermolecular interaction energies of the studied compounds with *E. coli* peptide deformylase

No.	E_{min}	No.	E_{min}	No.	E_{min}	No.	E_{min}	No.	E_{min}
1	-7.3	**3**	-7.1	**5**	-7.8	**7**	-7.6	**9**	-7.8
2	-7.4	**4**	-6.7	**6**	-6.9	**8**	-7.9	**10**	-6.8
Actinonin	-6.7								

Table 12. Nature and types of interactions of the studied compounds with amino acid residues of *E. coli* peptide deformylase

No.	Types of interactions and amino acid residues
1	ILE B:93 (conventional H bond), CYS B:90 (conventional H bond), PRO B:94(π-donor H bond, C-H bond), ARG B:97 (π-anion, π-cation), LEU B:91 (alkyl, π-alkyl), GLU B:95 (π-donor H bond, C-H bond), HIS B:7 (alkyl, π-alkyl), GLU B:41 (π-anion, π-cation)
2	GLY B:89 (C-H bond), ARG B:97 97 (conventional H bond, π-cation), ILE B:44 (π-σ), PRO B:94 (alkyl, π-alkyl), LEU B:91 (alkyl, π-alkyl)
3	GLY B:89 (C-H bond), ILE B:44 (π-σ, π-alkyl), ARG B:97 (π-cation).
4	GLU B:95 (C-H bond), PRO B:94 (alkyl, π-alkyl), GLU B:41(π-anion), ARG B:97 (π-cation), ILE B:44 (alkyl, π-alkyl), HIS B:7 (alkyl, π-alkyl)
5	GLU B:41 (π-donor H bond, C-H bond), GLY B:89 (π-donor H bond, C-H bond), GLU B:95 (π-donor H bond, C-H bond), ARG B:97 (conventional H bond, π-cation), ILE B:44 (π-σ, π-alkyl)
6	ARG B:97(conventional H bond, π-cation), ILE B:44 (alkyl), GLY B:89 (conventional H bond)
7	ILE B:44 (π-σ), ARG B:97 (conventional H bond, π-cation), GLY B:89 (π-donor H bond, C-H bond), LEU B:125 (alkyl), ILE B:86 (alkyl), LEU B:91 (alkyl), PRO B:94 (alkyl), GLU B:95 (π-donor H bond, C-H bond)
8	CYS B:90 (conventional H bond), GLU B:95 (conventional H bond, π-donor H bond), GLU B:41 (π-anion), PRO B:94 (π-alkyl), ARG B:97 (conventional H bond), LEU B:91 (π-alkyl)
9	GLU B:95 (conventional H bond), GLN B:96 (conventional H bond), CYS B:90 (conventional H bond), ILE B:44 (π-σ, π-alkyl), LEU B:91 (π-alkyl)
10	GLU B:41 (π-donor H bond, C-H bond), GLY B:89 (π-donor H bond, C-H bond), ILE B:44 (π-σ), ARG B:97 (conventional H bond, π-cation)

compounds **8** (-7.9 kcal/mol), **5** and **9** (-7.8 kcal/mol), exceeding that of the reference inhibitor actinonin (-6.7 kcal/mol). Compounds **1–3** and **7** demonstrated moderate affinity (-7.1 kcal/mol to -7.6 kcal/mol), while compounds **4, 6** and **10** exhibited E_{min} values (-6.7 kcal/mol to -6.9 kcal/mol) comparable to the reference molecule.

Molecular docking with *E. coli* PDF demonstrated the formation of stable complexes through a broad spectrum of non-covalent interactions, predominantly hydrogen bonds, π-interactions (π-σ, π-alkyl, π-cation, π-donor, π-anion), and hydrophobic contacts *(Table 12)*. The residue ARG B:97 played a key role in complex stabilization, participating in both π-cation and hydrogen bonding interactions, alongside ILE B:44, GLU B:95, GLY B:89, LEU B:91, PRO B:94, CYS B:90 and GLU B:41. Compound **1** exhibited the most diverse interaction profile (π-σ, π-cation, H-bonds, alkyl), consistent with its high binding affinity. Compounds **5–7** formed numerous hydrogen bonds with CYS B:90, GLU B:95 and GLN B:96, whereas the remaining structures (**2**–**4, 6, 10**) displayed a more limited range of interactions but maintained complex stability through π- and hydrogen-bonding interactions with key residues.

Molecular docking with *S. aureus* PDF demonstrated higher binding affinities for all studied compounds compared to the reference inhibitor actinonin (-6.7 kcal/mol). The lowest binding energy (-8.8 kcal/mol) was observed for compound **5**, while compounds **8–10** exhibited similar values (-8.5 kcal/mol to -8.4 kcal/mol). Compounds **1–4** and **7** displayed binding energies of -7.6 kcal/mol to -8.3 kcal/mol, whereas compound **6** showed the lowest affinity among the studied derivatives (-7.5 kcal/mol), yet still exceeded that of actinonin *(Table 13)*.

Molecular docking with *S. aureus* peptide deformylase demonstrated that all studied compounds form multiple non-covalent contacts with active site amino acid residues, resulting in high binding affinity and potential biological activity *(Table 14)*. The primary interactions are hydrophobic contacts (alkyl and π-alkyl) with VAL A:59, VAL A:151, LEU A:105, LEU A:112 and PRO A:78, as well as T-shaped π-π interactions with HIS A:154. Hydrogen bonds (TYR A:147, SER A:57, ARG A:56, GLY A:110) and electrostatic interactions, including π-anion/π-cation contacts with GLU A:185, play an important role in enhancing specificity. Halogen interactions were also observed for certain compounds (e. g., compound **6**).

Molecular docking of the studied derivatives with anaplastic lymphoma kinase (ALK) demonstrated their ability to form stable complexes with the enzyme's active site. Although none of the compounds exceeded the binding affinity of the reference inhibitor crizotinib (-9.4 kcal/mol), the closest in binding energy were compounds **2, 5** and **10** (-8.7 kcal/mol to -8.9 kcal/mol), as well as **6** and **9** (-8.6 kcal/mol) *(Table 15)*. The remaining structures exhibited moderate affinity (-7.5 kcal/mol to -8.1 kcal/mol).

Docking analysis with the ALK active site demonstrated the formation of ligand-receptor complexes through a broad spectrum of interactions *(Table 16)*. The primary interactions are hydrophobic contacts (alkyl and π-alkyl) with LEU A:1122, LEU A:1256, LEU A:1196, ALA A:1148, VAL

Table 13. Intermolecular interaction energies of the studied compounds with peptide deformylase (*S. aureus*)

No.	E_{min}	No.	E_{min}	No.	E_{min}	No.	E_{min}	No.	E_{min}
1	-8.1	**3**	-7.6	**5**	-8.8	**7**	-8.3	**9**	-8.5
2	-8.2	**4**	-7.8	**6**	-7.5	**8**	-8.4	**10**	-8.4
Actinonin	-6.7								

Table 14. Nature and types of interactions of the studied compounds with amino acid residues of *S. aureus* peptide deformylase

No.	Types of interactions and amino acid residues
1	TYR A:147 (conventional H bond), VAL A:151 (π-σ), LEU A:112 (alkyl, π-alkyl), ARG A:56 (alkyl, π-alkyl), VAL A:59 (alkyl, π-alkyl)
2	SER A:57 (conventional H bond), LEU A:112 (π-alkyl), GLU A:185 (π-anion), VAL A:151 (π-alkyl), VAL A:59 (π-alkyl), LEU A:105 (π-alkyl)
3	HIS A:154 (π-π T-shaped), VAL A:151(alkyl, π-alkyl), LEU A:105 (alkyl, π-alkyl), PRO A:78 (alkyl, π-alkyl), VAL A:59 (alkyl, π-alkyl), GLU A:185 (C-H bond, π-anion), SER A:57 (conventional H bond)
4	GLY A:58 (C-H bond), VAL A:59 (π-σ), HIS A:154 (π-π T-shaped), VAL A:151 (alkyl, π-alkyl), ILE A:150 (alkyl, π-alkyl), LEU A:112 (alkyl, π-alkyl), ARG A:56 (alkyl, π-alkyl), LEU A:105 (alkyl, π-alkyl)
5	VAL A:151 (π-alkyl), GLU A:185 (attractive charge), LEU A:105 (π-alkyl), ARG A:56 (conventional H bond, π-anion), LEU A:112 (π-alkyl)
6	GLU A:185 (halogen (Fluorine)), GLY A:110 (π-donor H bond), HIS A:154 154 (π-π T-shaped), VAL A:151 (π-alkyl)
7	VAL A:151 (π-alkyl), PRO A:78 (π-alkyl), TYR A:147 (conventional H bond), HIS A:154 (π-π T-shaped), GLU A:185 (attractive charge), VAL A:59 (π-alkyl)
8	ILE A:150 (C-H bond), GLY A:58 (C-H bond), HIS A:154 (π-σ), GLU A:185 (attractive charge), LEU A:112 (π-alkyl), VAL A:59 (π-alkyl), ARG A:56 (conventional H bond)
9	HIS A:154 (π-donor H bond), VAL A:59 (π-alkyl), GLU A:185 (π-anion), VAL A:151 (π-alkyl), LEU A:112 (π-alkyl), SER A:57 (conventional H bond), LEU A:105 (π-alkyl)
10	LEU A:105 (π-alkyl), GLU A:185 (π-cation), LEU A:112 (π-alkyl), VAL A:151 (C-H bond, π-donor H Bond), ARG A:56 (conventional H Bond, attractive charge), HIS A:154 (C-H bond, π-donor H Bond)

Table 15. Intermolecular interaction energies of the studied compounds with ALK

No.	E_{min}	No.	E_{min}	No.	E_{min}	No.	E_{min}	No.	E_{min}
1	-7.5	**3**	-8.1	**5**	-8.7	**7**	-7.9	**9**	-8.6
2	-8.9	**4**	-7.9	**6**	-8.6	**8**	-8.0	**10**	-8.7
Crizotinib	-9.4								

Table 16. Nature and types of interactions with ALK

No.	Types of interactions and amino acid residues
1	LEU A:1256 (π-σ), VAL A:1130 (alkyl, π-alkyl), ARG A:1253 (alkyl, π-alkyl), ASP A:1270 (attractive charge, π-cation), LEU A:1122 (alkyl, π-alkyl), LYS A:1150 (attractive charge, π-cation)
2	ASP A:1203 (attractive charge, conventional H bond), LEU A:1256 (π-alkyl), ALA A:1148 (π-alkyl), LEU A:1122 (π-σ), VAL A:1130 (π-alkyl)
3	ASP A:1203 (salt bridge, conventional H bond), LEU A:1122 (C-H bond), ALA A:1148 (π-alkyl), LEU A:1256 (π-σ), VAL A:1130 (π-alkyl)
4	LEU A:1196 (alkyl, π-alkyl), VAL A:1130 (alkyl, π-alkyl), ASP A:1203 (attractive charge), LEU A:1256 (π-σ), ALA A:1148 (alkyl, π-alkyl), GLY A:1202 (C-H bond), ASN A:1254 (C-H bond), LEU A:1122 (alkyl, π-alkyl)
5	LEU A:1122 (conventional H bond), ASP A:1203 (attractive charge, π-anion), ASP A:1270 (attractive charge, π-anion), ASN A:1254 (halogen (fluorine)), VAL A:1130 (π-alkyl), GLY A:1269 (halogen (fluorine)), LEU A:1256 (π-alkyl), ALA A:1148 (π-alkyl)
6	ARG A:1253 (C-H bond, halogen (fluorine)), ALA A:1148 (π-alkyl), ASP A:1270 (π-anion), LEU A:1256 (π-σ), VAL A:1130 (π-alkyl)
7	ASP A:1203 (attractive charge, conventional H bond), LEU A:1122 (conventional H bond, π-σ, alkyl, π-alkyl), ARG A:1253 (alkyl, π-alkyl), LEU A:1196 (alkyl, π-alkyl), ALA A:1148 (alkyl, π-alkyl), VAL A:1130(alkyl, π-alkyl), LEU A:1256(alkyl, π-alkyl)
8	ASP A:1203 (attractive charge, π-anion), VAL A:1130 (π-σ), LEU A:1196 (π-σ), LYS A:1150 (alkyl, π-alkyl), ALA A:1148 (alkyl, π-alkyl), LEU A:1122 (alkyl, π-alkyl), LEU A:1256 (alkyl, π-alkyl), MET A:1199 (C-H bond), ASP A:1270 (attractive charge, π-anion), ALA A:1126 (alkyl, π-alkyl)
9	ASP A:1203 (attractive charge, π-anion), LEU A:1122 (π-alkyl), ASP A:1270 (attractive charge, π-anion), LEU A:1256 (π-alkyl), ALA A:1148 (π-alkyl), VAL A:1130 (π-alkyl)
10	LEU A:1256 (π-σ), VAL A:1130 (alkyl, π-alkyl), ARG A:1253 (alkyl, π-alkyl), ASP A:1270 (attractive charge, π-cation), LEU A:1122 (alkyl, π-alkyl), LYS A:1150 (attractive charge, π-cation)

A:1130 and ARG A:1253, which stabilize the molecules within the protein's hydrophobic pocket. Electrostatic and π-anion interactions with ASP A:1203 and ASP A:1270 play a significant role and are characteristic for most compounds (**2, 3, 5, 7–9**). Additional H-bonds were observed for compounds **2, 3, 5** and **7** (ASP A:1203, LEU A:1122, ASN A:1254), while compounds **5, 6** and **8** exhibited halogen and π-σ interactions (LEU A:1256, VAL A:1130). The most promising derivatives were **2, 5, 8** and **9**, forming an extensive network of specific and non-specific contacts, indicative of their high potential as ALK inhibitors.

Discussion

According to the results of the comparative in silico analysis, the toxicological profile of the 1,2,4-triazolo[1',5':1,6] pyrido[3,4-*b*]indole derivatives is largely determined by the electronic properties and the position of substituents in the benzylidene fragment. Halogenated derivatives (**5–7**) exhibit lower acute toxicity in warm-blooded animals but higher ecotoxicity, likely due to their lipophilicity and tendency for bioaccumulation. Methoxy-substituted derivatives (**3**, **4**) showed intermediate toxicity, whereas nitro-substituted compounds (**9**, **10**) pose a higher risk to warm-blooded organisms, consistent with the known effects of nitro groups on biological activity. Compound **8** combines moderate toxicity for warm-blooded organisms with low toxicity for aquatic species, attributable to the hydrophilicity of the tertiary amine, while the unsubstituted compound **1** demonstrates the highest safety profile, despite a positive mutagenicity prediction. Overall, halogenation reduces toxicity for warm-blooded animals but increases ecological risk; electron-donating groups (-OCH_3, -$N(CH_3)_2$) reduce both types of toxicity; nitro-groups increase risk for both warm-blooded organisms and ecosystems.

ADME analysis indicated that most of the investigated derivatives comply with key pharmacokinetic parameters. Compounds with lower molecular weight and limited conformational flexibility (**1**, **2**, **5–7**) potentially exhibit better bioavailability and BBB permeability, whereas more polar derivatives (**3**, **4**, **10**) may have limited permeability but enhanced selectivity toward protein targets. Limited solubility of most structures may restrict their bioavailability; compound 1 stands out with the most favorable combination of solubility and pharmacokinetic properties. Excessive lipophilicity of certain derivatives (**6**, **7**) may promote bioaccumulation, while the hydrophilicity of compound **1** limits passive absorption.

High predicted gastrointestinal absorption supports the suitability of these compounds for oral administration, whereas low transdermal permeability indicates limited potential for transdermal formulations. Observed substrate activity toward P-glycoprotein (P-gp) and inhibition of CYP3A4 and CYP2D6 suggest potential drug – drug interactions, whereas the absence of such activity in compound **1** is advantageous.

All derivatives demonstrate an acceptable drug-likeness profile, conforming to Lipinski's rules as well as additional criteria, although deviations from the Muegge filter indicate potential risks related to lipophilicity and solubility. Predicted oral bioavailability (0.55) is adequate; however, PAINS and Brenk alerts highlight the need for further toxicological evaluation, particularly for compounds **1**, **9** and **10**.

Molecular docking showed that the investigated structures can potentially bind stably to the active sites of multiple targets. For COX-2, all compounds demonstrate moderate activity, with compound **6** exhibiting the lowest binding energy, while compounds **4**, **5**, **9** and **10** also appear promising. In the case of CYP51, compounds **2**, **5**, **8** and **10** are notable, displaying binding energies comparable to fluconazole, indicating potential as antifungal agents.

Docking with *E. coli* PDF confirmed high affinity for all derivatives, with compounds **5**, **8** and **9** surpassing actinonin in complex stability. ARG B:97 plays a key role in ligand anchoring, complemented by hydrophobic and electrostatic interactions from surrounding residues. A similar trend is observed for *S. aureus* PDF, where compounds **5**, **8–10** outperform the reference inhibitor, highlighting their antimicrobial potential.

For ALK kinase, compounds **2**, **5**, **6**, **9** and **10** show affinity levels comparable to crizotinib, suggesting potential as antitumor agents. Although the reference drug exhibits more favorable energetic characteristics, the identified lead structures may serve as a basis for further structural optimization to enhance specificity and efficacy.

Conclusions

1. The conducted *in silico* modeling demonstrated that the 1,2,4-triazolo[1′,5′:1,6]pyrido[3,4-*b*]indole derivatives possess a favorable toxicological and pharmacokinetic profile, comply with drug-likeness criteria, and exhibit high predicted gastrointestinal absorption with limited central nervous system penetration.

2. Molecular docking confirmed their significant potential as inhibitors of COX-2, CYP51, peptide deformylases and ALK kinase, with several compounds showing binding affinities comparable to or exceeding those of reference inhibitors.

3. These findings highlight the promise of these derivatives as multitarget drug candidates with antibacterial, antitumor, and anti-inflammatory activities, supporting their further structural optimization and preclinical investigation.

Funding
The study was performed without financial support.

Conflicts of interest: authors have no conflict of interest to declare.
Конфлікт інтересів: відсутній.

Information about the authors:
Fedotov S. O., PhD, Senior Lecturer of the Department of Toxicological and Inorganic Chemistry, Zaporizhzhia State Medical and Pharmaceutical University, Ukraine.
ORCID ID: 0000-0002-0421-5303
Hotsulia A. S., PhD, DSc, Professor of the Department of Toxicological and Inorganic Chemistry, Zaporizhzhia State Medical and Pharmaceutical University, Ukraine.
ORCID ID: 0000-0001-9696-221X

Відомості про авторів:
Федотов С. О., д-р філософії, старший викладач каф. токсикологічної та неорганічної хімії, Запорізький державний медико-фармацевтичний університет, Україна.
Гоцуля А. С., д-р фарм. наук, професор каф. токсикологічної та неорганічної хімії, Запорізький державний медико-фармацевтичний університет, Україна.

Andrii Hotsulia (Андрій Гоцуля)
andrey.goculya@gmail.com

References

1. Elrashedy A, Ibrahim NE, Abo-Salem H, Elaasser MM, El-Sawy ER. Design, synthesis, and molecular modeling of new 1,2,4-triazole-containing indole compounds as aromatase antagonists for the treatment of breast cancer. Bioorg Chem. 2025;163:108677. doi: 10.1016/j.bioorg.2025.108677
2. Rohilla S, Goyal G, Berwal P, Mathur N. A Review on Indole-triazole Molecular Hybrids as a Leading Edge in Drug Discovery: Current Landscape and Future Perspectives. Curr Top Med Chem. 2024;24(18):1557-88. doi: 10.2174/0115680266307132240509065351
3. Berwal P, Rohilla S, Mathur N, Rani K. Synthesis, Molecular Docking, and Biological Evaluation of Novel Indole-triazole Conjugates. Curr Drug Discov Technol. 2024;21(6):e120324227917. doi: 10.2174/011570163829573924022207442 6
4. Mahmoud E, Abdelhamid D, Mohammed AF, Almarhoon ZM, Bräse S, Youssif BG, et al. Design, Synthesis, and Antiproliferative Activity of Novel Indole/1,2,4-Triazole Hybrids as Tubulin Polymerization Inhibitors. Pharmaceuticals (Basel). 2025;18(2):275. doi: 10.3390/ph18020275
5. Pravin NJ, Kavalapure RS, Alegaon SG, Gharge S, Ranade SD. Indoles as promising Therapeutics: A review of recent drug discovery efforts. Bioorg Chem. 2025;154:108092. doi: 10.1016/j.bioorg.2024.108092
6. Shcherbyna R, Panasenko O, Polonets O, Nedorezanıuk N, Duchenko M. Synthesis, antimicrobial and antifungal activity of ylidenhydrazides of 2-((4-R-5-R_1-4H-1,2,4-triazol-3-yl)thio)acetaldehydes. Journal of Faculty of Pharmacy of Ankara University. 2021;45(3):504-14. doi: 10.33483/jfpau.939418
7. Dovbnia DV, Kaplaushenko AH, Frolova YS. A study of hypoglycemic activity of acids and salts containing 1,2,4-triazole. Ceska Slov Farm. 2023;72:113-24. https://www.prolekare.cz/casopisy/ceska-slovenska-farmacie/2023-3-11/studium-hypoglykemickej-aktivity-kyselin-a-soli-obsahujucich-1-2-4-triazol-135087/
8. Safonov A. Method of synthesis novel N'-substituted 2-((5-(thiophen-2-ylmethyl)-4H-1,2,4-triazol-3-yl)thio)acetohydrazides. Journal of Faculty of Pharmacy of Ankara University. 2020;44(2):242-52. doi: 10.33483/jfpau.580011
9. Gotsulya A, Fedotov S, Zinych O, Trofimova T, Brytanova T. Synthesis and properties of S-alkyl 4-(4-chlorophenyl)-5-(pyrrole-2-yl)-1,2,4-triazole-3-thiol derivatives. Journal of Faculty of Pharmacy of Ankara University. 2023;47(3):1020-32. doi: 10.52794/hujpharm.1011368
10. Karpenko Y, Hunchak Y, Gutyj B, Hunchak A, Parchenko M, Parchenko V. Advanced research for physico-chemical properties and parameters of toxicity piperazinium 2-((5-(furan-2-yl)-4-phenyl-4*H*-1,2,4-triazol-3-yl)thio)acetate. ScienceRise: Pharmaceutical Science. 2022;2(36):18-25. doi: 10.15587/2519-4852.2022.255848
11. Demchenko S, Lesyk R, Yadlovskyi O, Holota S, Yarmoluk S, Tsyhankov S, et al. Fused triazole-azepine hybrids as potential non-steroidal antiinflammatory agents. Scientia Pharmaceutica. 2023;91(2):26. doi: 10.3390/scipharm91020026
12. Toxicity Estimation Software Tool (TEST) [Internet]. US EPA. 2020 [cited 2025 Sep19]. Available from: https://www.epa.gov/comptox-tools/toxicity-estimation-software-tool-test
13. Ahmadi M, Bekeschus S, Weltmann KD, von Woedtke T, Wende K. Non-steroidal anti-inflammatory drugs: recent advances in the use of synthetic COX-2 inhibitors. RSC Med Chem. 2022;13(5):471-96. doi: https://doi:10.1039/d1md00280e
14. Biovia. Discovery Studio Visualizer, v 19.1.0.18287 [Software]. 2019 [cited 2025 Sep19]. Available from: https://www.3ds.com/products/biovia
15. ChemAxon. MarvinSketch, Version 6.3.0 [Software]. 2015 [cited 2025 Sep19]. Available from: http://www.chemaxon.com
16. Worldwide Protein Data Bank. Protein Data Bank (PDB) [Database]. [cited 2025 Sep19]. Available from: http://www.pdb.org